Intracellular pH Regulation by Na^+/H^+ Exchange Requires Phosphatidylinositol 4,5-Bisphosphate

Orit Aharonovitz,* Hans C. Zaun,‡ Tamas Balla,§ John D. York,‖ John Orlowski,‡ and Sergio Grinstein*

*Cell Biology Programme, Research Institute, The Hospital for Sick Children, Toronto, Ontario M5G 1X8, Canada; ‡Department of Physiology, McGill University, Montréal, Québec, H3G 1Y6, Canada; §Endocrinology and Reproduction Research Branch, National Institutes of Child Health and Human Development, National Institutes of Health, Bethesda, Maryland 20892-4510; and ‖Department of Pharmacology and Cancer Biology, Duke University Medical Center, Durham, North Carolina 27710

Abstract. The carrier-mediated, electroneutral exchange of Na^+ for H^+ across the plasma membrane does not directly consume metabolic energy. Nevertheless, acute depletion of cellular ATP markedly decreases transport. We analyzed the possible involvement of polyphosphoinositides in the metabolic regulation of NHE1, the ubiquitous isoform of the Na^+/H^+ exchanger. Depletion of ATP was accompanied by a marked reduction of plasmalemmal phosphatidylinositol 4,5-bisphosphate (PIP_2) content. Moreover, sequestration or hydrolysis of plasmalemmal PIP_2, in the absence of ATP depletion, was associated with profound inhibition of NHE1 activity. Examination of the primary structure of the COOH-terminal domain of NHE1 revealed two potential PIP_2-binding motifs. Fusion proteins encoding these motifs bound PIP_2 in vitro. When transfected into antiport-deficient cells, mutant forms of NHE1 lacking the putative PIP_2-binding domains had greatly reduced transport capability, implying that association with PIP_2 is required for optimal activity. These findings suggest that NHE1 activity is modulated by phosphoinositides and that the inhibitory effect of ATP depletion may be attributable, at least in part, to the accompanying net dephosphorylation of PIP_2.

Key words: amiloride • ATP depletion • Na^+/H^+ antiport • phosphoinositide

Introduction

Na^+/H^+ exchangers (NHEs)[1] are a family of electroneutral antiporters that play an essential role in the regulation of the intracellular pH (pH_i) and cell volume, and also mediate transepithelial Na^+ and HCO_3^- absorption (for reviews see Orlowski and Grinstein, 1997; Aharonovitz and Grinstein, 1999). Fluxes through the NHE are driven solely by the combined chemical gradients of Na^+ and H^+ and, hence, do not directly consume metabolic energy (Kinsella and Aronson, 1980). Nevertheless, the presence of physiological levels of ATP is required for optimal Na^+/H^+ exchange in all cases studied to date (Cassel et al., 1986; Brown et al., 1991; Kapus et al., 1994; Levine et al., 1993). Procedures that reduce intracellular ATP drastically inhibit Na^+/H^+ exchange in a variety of native systems (Cassel et al., 1986; Brown et al., 1991), as well as in antiport-deficient cells transfected with either NHE1, 2, or 3 (Levine et al., 1993; Kapus et al., 1994). Metabolic depletion depresses the rate of transport, at least in some instances, by reducing the affinity of the exchangers for intracellular H^+, without altering the number of plasmalemmal transporters.

The pronounced inhibition of exchange activity induced by metabolic depletion is not accompanied by detectable alterations in the phosphorylation of the antiporter (Goss et al., 1994). Moreover, in the case of the ubiquitous isoform NHE1, the sensitivity to ATP persists after elimination of virtually all the putative phosphorylation sites by mutagenesis (Goss et al., 1994; Wakabayashi et al., 1994). Comparable studies have not been reported for other isoforms, but NHE3 remains sensitive to ATP even after truncation of a large part of its cytosolic domain, where most of the phosphorylation sites reside (Cabado et al.,

---

Address correspondence to Sergio Grinstein, Division of Cell Biology, Hospital for Sick Children, 555 University Avenue, Toronto, M5G 1X8, Canada. Tel.: (416) 813-5727. Fax: (416) 813-5028. E-mail: sga@sickkids.on.ca

[1]*Abbreviations used in this paper:* AM, acetoxymethylester; BCECF, $2',7'$-bis(2-carboxyethyl)-5(6)-carboxyfluorescein; Ca^{2+}_i, cytosolic free calcium; ERM, ezrin/radixin/moesin; GFP, green fluorescent protein; GST, glutathione-S-transferase; IP_3, 1,4,5,-trisphosphate; HA, hemagglutinin; NHE, Na^+/H^+ exchanger; NMG, *N*-methyl-D-glucammonium; pH_i, intracellular pH; PH, pleckstrin homology; PIP_2, phosphatidylinositol-4,5-bisphosphate; PLC, phospholipase C; TPCK, *N*-tosyl-l-phenylalanine chloromethyl ketone.

1996). In view of these findings, direct phosphorylation appears unlikely to account for the ATP dependence of the exchangers and alternative mechanisms must be considered.

Associated proteins or lipids are likely to play a role in the control of NHE activity. Such ancillary components may themselves be subject to phosphorylation, perhaps accounting for the observed ATP dependence of Na^+/H^+ exchange. Indeed, a variety of proteins have been proposed to bind to NHE1, including calmodulin (Bertrand et al., 1994), HSP70 (Silva et al., 1995), and CHP, a calcineurin homologue (Lin and Barber, 1996). Similarly, NHERF-1 and 2 have been shown to interact directly with NHE3 (Weinman et al., 1993; Yun et al., 1997). While direct phosphorylation of NHERF by protein kinase A was initially postulated to account for its effects on the activity of NHE3 (Weinman et al., 1993), this conclusion was subsequently revised (Zizak et al., 1999). Therefore, to date, there is no conclusive evidence that protein phosphorylation is responsible for the ATP sensitivity of the NHE isoforms.

Polyphosphoinositides are ubiquitous constituents of animal plasma membranes, where they have been found to exert modulatory effects on the activity of several ion transporters. Thus, optimal activity of K^+ channels (Hilgemann and Ball, 1996; Baukrowitz et al., 1998) and Na^+/Ca^{2+} antiporters (Hilgemann and Ball, 1996) was found to require the presence of phosphatidylinositol-4,5-bisphosphate (PIP_2). Because phosphorylation of polyphosphoinositides is in a dynamic equilibrium, depletion of cellular ATP is anticipated to favor net dephosphorylation of inositol phospholipids, reducing the concentration of the most highly phosphorylated species, particularly PIP_2. Therefore, the ATP sensitivity of transporters, including NHE, could be attributable to alterations in the cellular content of PIP_2 (Hilgemann and Ball, 1996; Baukrowitz et al., 1998).

Binding of channels and exchangers to PIP_2 is thought to be mediated, at least in some cases, by a characteristic motif comprised of cationic and hydrophobic amino acids (Huang et al., 1998). This linear sequence was initially identified in actin-binding proteins such as gelsolin and profilin, which are themselves regulated by polyphosphoinositides (Yu et al., 1992). Interestingly, two related motifs can be discerned in the cytosolic domain of NHE1 (in rats, residues 513–520 and 556–564). This observation raised the possibility that NHE1 may interact physically and functionally with phosphoinositides. The purpose of the experiments described in this report was threefold: (1) to determine if alterations in the cellular content of PIP_2 are associated with the inhibition of NHE1 observed upon ATP depletion; (2) to assess whether the cytosolic domain of NHE1 can specifically bind to PIP_2; and (3) to define whether such binding is required for optimal NHE1 activity.

Materials and Methods

Materials and Solutions

Nigericin, 2′,7′-bis(2-carboxyethyl)-5(6)-carboxyfluorescein (BCECF) acetoxymethylester (AM), Fura-2-AM, and rhodamine-phalloidin were ob-

tained from Molecular Probes, Inc. Chymotrypsin, N-tosyl-L-phenylalanine chloromethyl ketone (TPCK), 2-deoxy-D-glucose, antimycin A, sulfinpyrazone, PIP_2, and the substrate for detection of peroxidase activity (Sigma Fast OPD) were from Sigma Chemical Co. Paraformaldehyde was purchased from Canemco Inc., and Triton X-100 was from Bio-Rad Laboratories. Mouse mAbs to PIP_2 were obtained from PerSeptive Biosystems, Inc. Mouse mAbs to influenza virus hemagglutinin (HA) peptide were obtained from BAbCo. HRP-coupled goat anti–mouse antibodies were from Jackson ImmunoResearch Laboratories. Enhanced chemiluminescence reagents were from Amersham International. Fatty acid–free BSA and the ATP assay kit were purchased from Calbiochem. A peptide corresponding to amino acids 550–564 of NHE1 was synthesized by Sheldon Biotechnology Center (McGill University, Montreal, Quebec). All other chemicals were of analytical grade and were obtained from Aldrich Chemical Co.

The isotonic Na^+-rich medium contained (in mM): 140 NaCl, 5 KCl, 1 $CaCl_2$, 1 $MgCl_2$, 10 glucose, and 10 Hepes-Na$^+$, pH 7.4. Isotonic Na^+-free medium contained (in mM): 140 KCl, 1 $CaCl_2$, 1 $MgSO_4$, 5.5 glucose, and 25 N-methyl-D-glucammonium (NMG)-Hepes, pH 7.4. PBS contained (in mM): 150 NaCl, 10 KCl, 8 sodium phosphate, and 2 potassium phosphate, pH 7.4. TBS contained (in mM): 150 NaCl and 20 Tris-HCl, pH 7.4.

cDNA Construction and Transfection

A vector for expression of a chimeric protein consisting of the pleckstrin homology (PH) domain of phospholipase C_δ (PLCδ and enhanced green fluorescent protein [GFP]), termed PH$_{PLC\delta}$-GFP, was constructed as reported earlier (Varnai and Balla, 1998). PH$_{PLC\delta}$-GFP cDNA was transfected into AP-1 cells stably expressing wild-type rat NHE1$'_{HA}$ (AP-1/NHE1$'_{HA}$; described below) by the calcium phosphate coprecipitation method of Chen and Okayama (1988). A vector for expression of the myristoylated and palmitoylated form of Inp54p, a yeast PIP_2-specific 5′-phosphatase, fused to GFP and, termed PM-5′-phosphatase-GFP, was constructed as reported earlier (Raucher et al., 2000). PM-5′-phosphatase-GFP and PH$_{PLC\delta}$-GFP cDNA was transfected into COS-1 cells using FuGENE™ 6 transfection reagent (Roche Diagnostics Corp., Indianapolis, IN).

The rat NHE1 cDNA, engineered to contain a series of unique restriction endonuclease sites for subcloning purposes, was inserted into a mammalian expression vector under the control of the enhancer/promoter region from the immediate early gene of human cytomegalovirus (plasmid called pNHE1′), as previously described (Orlowski and Kandasamy, 1996). To facilitate immunological detection of the protein, the influenza virus HA epitope YPYDVPDYAS, preceded by a single G amino acid linker (added to create peptide flexibility), was inserted at the very COOH-terminal end of NHE1′ using the PCR. In control experiments, these modifications had no obvious effect on the basal activity or functional properties of NHE1 (called NHE1$'_{HA}$) when expressed in AP-1 cells (described below). Individual and combined mutations of two putative PIP_2-binding motifs (termed M1 and M2) in NHE1$'_{HA}$ were accomplished using a commercially available, PCR mutagenesis procedure (QuikChange site-directed mutagenesis kit, Stratagene). Clusters of positively charged residues in the M1 (^{513}KKKQETKR^{520}) and the M2 (^{556}RFNKKYVKK^{564}) motifs were substituted with alanine, i.e., ^{513}AAAQETAA^{520} and ^{556}AFNAAYVAA^{564}, respectively. The cDNAs were sequenced to confirm the presence of the mutations and to ensure that other random mutations were not introduced.

Cell Lines

COS-1 cells were obtained from American Type Culture Collection. WT5 is a subline of wild-type CHO cells. AP-1, a cell line devoid of endogenous Na^+/H^+ exchange activity, was isolated from WT5 cells as previously described (Rotin and Grinstein, 1989). AP-1 cells were transfected with plasmids containing the wild-type and mutant NHE1$'_{HA}$ constructs by the calcium phosphate–DNA coprecipitation technique of Chen and Okayama (1988). Starting 48 h after transfection, the AP-1 cells were selected for survival in response to repeated (5–6 times over a 2-wk period) acute NH_4Cl-induced acid loads (Orlowski, 1993) to discriminate between NHE-positive and negative transfectants.

pH$_i$ Determinations

Na^+-induced changes of pH$_i$ were measured fluorimetrically using BCECF, essentially as described (Grinstein et al., 1992). In brief, cells

grown to 60–70% confluence on glass coverslips were loaded with 2 μg/ml of BCECF-AM for 10 min at 37°C in Na$^+$-rich medium. Two methods were used to measure the fluorescence of BCECF. For population measurements, the coverslip was placed in a thermostated Leiden holder on the stage of a Nikon TMD-Diaphot microscope equipped with a Nikon Fluor oil immersion objective and Hoffman modulation optics. A chopping mirror was used to direct the excitation light alternately to two excitation filters (490BP10 and 440BP10 nm) in front of a xenon lamp. To minimize dye bleaching and photodynamic damage, neutral density filters were used to reduce the intensity of the excitation light reaching the cells. The excitation light was directed to the cells via a 510-nm dichroic mirror, and fluorescence emission was collected through a 535BP25 nm filter. Photometric data were acquired at 10 Hz using Oscar software (Photon Technologies Inc.).

The fluorescence of transiently transfected single cells was measured using a ratio imaging system controlled by the Metafluor software (Universal Imaging), essentially as previously described (Gan et al., 1998). Transfected cells were identified by detecting GFP fluorescence before loading with BCECF. A neutral density filter was interposed in the excitation pathway, to decrease the signal emanating from GFP, and the cells were loaded with BCECF while on the microscope stage. The fluorescence of BCECF greatly exceeded that of GFP and was readily visible in the presence of the neutral density filter.

An acute acid load was imposed by preincubating the cells with 20 mM (NH$_4$)$_2$SO$_4$ for 10 min, followed by five rapid washes in NH$_4^+$- and Na$^+$-free solution. The rate of pH$_i$ recovery was measured upon reintroduction of isotonic Na$^+$-rich medium. Calibration of the fluorescence ratio versus the pH was performed for each experiment using nigericin- and K$^+$-rich solutions of varying pH, as before (Kapus et al., 1994).

Cytosolic Free Calcium ([Ca^{2+}]$_i$) Measurements

To measure [Ca^{2+}]$_i$, AP-1/NHE1$'_{HA}$ cells were loaded with 1 μg/ml of Fura-2-AM for 15 min at 37°C in Na$^+$-rich medium containing 500 μM sulfinpyrazone. The fluorescence of Fura-2 was measured essentially as described above for BCECF, but using dual excitation with 340BP10- and 380BP10-nm filters, a 400-nm dichroic mirror and a 510BP25-nm emission filter. Unless indicated otherwise, all measurements of [Ca^{2+}]$_i$ were made in Na$^+$-rich medium without calcium.

Fluorescence Microscopy

To assess the formation of stress fibers, AP-1/NHE1$'_{HA}$ cells were plated onto coverslips and grown to 60–70% confluence. After washing three times with PBS, the cells were fixed for 40 min at room temperature using 4% paraformaldehyde in cold PBS containing 1 mM MgCl$_2$. After fixation, cells were washed twice with PBS and incubated with 100 mM glycine in PBS for 15 min. The coverslips were washed twice again, and the cells were permeabilized with 0.1% Triton X-100 in PBS for 15 min at room temperature. After washing three more times with PBS, the cells were incubated with a 1:500 dilution of rhodamine-phalloidin for 30 min. The coverslips were finally washed and mounted onto glass slides using DAKO mounting medium.

To estimate the amount of PIP$_2$ at the plasma membrane, AP-1/NHE1$'_{HA}$ cells were transfected with the PH$_{PLC\delta}$-GFP plasmid. After 48 h, the cells were treated as specified, immediately fixed and mounted as above. The localization of the fluorescent probe was examined with an LSM510 laser confocal microscope (Zeiss Inc.) using a 100× oil immersion objective. Digital images were analyzed using NIH Image software. To quantify fluorescence, regions of the cytosol or plasma membrane were enclosed by boxes and, after background subtraction, the intensity per unit area was determined. The ratio of plasmalemmal to cytosolic fluorescence is presented. In those cases where no defined plasmalemmal staining was discernible, the outermost layer of cytosolic fluorescence was used for the calculation, yielding a minimum ratio of ∼1.

^{22}Na$^+$ Influx Measurements

The cells were grown to confluence in 24-well plates. To examine the activity of the NHE as a function of the intracellular H$^+$ concentration, the pH$_i$ was clamped at different concentrations over the range of 5.4–7.4 by suspending the cells in media of varying K$^+$ concentrations containing the K$^+$/H$^+$ exchange ionophore nigericin (Thomas et al., 1979). The confluent monolayers were washed with isotonic NMG-chloride solution (140 mM NMG-chloride, 1 mM MgCl$_2$, 2 mM CaCl$_2$, 5 mM glucose, 10 mM Hepes,

pH 7.4), and incubated for 4 min at 22°C in NMG-balanced salt solutions specific for each pH$_i$ (pH-clamp solutions). All solutions contained 2 mM NaCl, 1 mM MgCl$_2$, 10 mM Hepes, pH 7.4, varying concentrations of K$^+$, and 10 μM nigericin. Additional components were included for the specified pH$_i$ values as follows (in mM): for pH$_i$ 7.4, 14 KCl, 126 potassium glutamate, 24 NMG-methane sulfonate; for pH$_i$ 7.0, 14 KCl, 42 potassium glutamate, 108 NMG-methane sulfonate; for pH$_i$ 6.6, 14 KCl, 8 potassium glutamate, 142 NMG-methane sulfonate; for pH$_i$ 6.2, 8.8 KCl, 155 NMG-methane sulfonate; for pH$_i$ 5.8, 3.6 KCl, 160 NMG-methane sulfonate; and for pH$_i$ 5.4, 1.4 KCl, 163 NMG-methane sulfonate. Because the rate of ATP consumption is likely to vary with pH, the ATP depletion procedure was initiated before acid loading. ^{22}Na$^+$ influx measurements were performed in the same K$^+$-nigericin solutions supplemented with ^{22}Na$^+$ (1 μCi/ml), 1 mM ouabain, and 0.1 mM bumetanide in the absence or presence of 2 mM amiloride. ^{22}Na$^+$ influx was linear with time for at least 10 min under these experimental conditions. Measurements of ^{22}Na$^+$ influx specific to the NHE were determined as the difference between the initial rates of H^+_i-activated ^{22}Na$^+$ influx in the absence and presence of 2 mM amiloride and expressed as amiloride-inhibitable ^{22}Na$^+$ influx.

The influx of ^{22}Na$^+$ was terminated by rapidly washing the cells three times with 4 vol of ice-cold NaCl stop solution (130 mM NaCl, 1 mM MgCl$_2$, 2 mM CaCl$_2$, 20 mM Hepes, pH 7.4). To extract the isotope, the monolayers were solubilized with 0.25 ml of 0.5 N NaOH, and the wells were washed with 0.25 ml of 0.5 N HCl. Both the NaOH cell extract and the HCl wash solution were combined in 5 ml scintillation fluid and transferred to scintillation vials. The radioactivity was assayed by liquid scintillation spectroscopy. Protein content was determined using the Bio-Rad DC protein assay kit according to the manufacturer's protocol. Each data point represents the average of at least three experiments, each performed in quadruplicate.

Depletion and Determination of ATP

Depletion of cellular ATP was carried out as described by Goss et al. (1994). In brief, AP-1/NHE1$'_{HA}$ cells were incubated for 10 min in a medium containing 100 mM K$^+$-glutamate, 30 mM KCl, 10 mM NaCl, 1 mM MgCl$_2$, 10 mM Hepes, pH 7.4, 5 mM 2-deoxy-D-glucose and 1 μg/ml antimycin A. This high K$^+$, low Na$^+$, and nominally Ca^{2+}-free medium was used to prevent Na$^+$ and/or Ca^{2+} loading of the cells upon inhibition of the Na$^+$/K$^+$ or Ca^{2+} pumps. Substitution of most of the Cl$^-$ by glutamate$^-$ was intended to minimize cell swelling. Cellular ATP content was determined using the Calbiochem assay kit. Cells (∼5 × 10^5) were extracted with 0.4 ml of 8% perchloric acid and placed on ice. The extract was neutralized with 1 M K$_2$CO$_3$, debris were sedimented, and aliquots of the supernatant (5 μl) were mixed with the buffer and luciferin–luciferase mixture provided by the kit's manufacturer. Sample luminescence was determined using a Beckman LS7000 counter and compared with ATP standards.

Quantification of Surface NHE1

We took advantage of the proteolytic susceptibility of NHE1 to quantify the fraction of the antiporters exposed at the cell surface, based on the earlier observations of Shrode et al. (1998). In brief, chymotryptic cleavage sites have been identified in the first and/or second putative extracellular loops of NHE1. When the protease is added to intact cells, cleavage at these sites can only be accomplished when NHE1 is inserted in the plasmalemma. This results in the disappearance of the fully glycosylated ∼105-kD band, corresponding to NHE1 in immunoblots. By contrast, the core-glycosylated immature form of NHE1 (∼80 kD), which resides in endomembranes, is unaffected by the protease, since under the conditions used chymotrypsin does not enter the cells. For these experiments AP-1/NHE1$'_{HA}$ cells, which were grown on 6-well plates, were incubated for 5 min at 37°C in the presence or absence of chymotrypsin (100 U/ml). Next, the cells were scraped off the wells with a rubber policeman and washed twice using Na$^+$-rich medium containing 100 μM TPCK. Finally, the cells were resuspended in Laemmli sample buffer and boiled for 5 min. Samples were subjected to electrophoresis in 7.5% polyacrylamide gels and transferred to nitrocellulose. Blots were blocked with 5% nonfat dried milk and exposed to a 1:5,000 dilution of mouse mAbs against HA. The secondary antibody, goat anti–mouse coupled to HRP, was used at 1:5,000 dilution. Immunoreactive bands were visualized using enhanced chemiluminescence. The amount of chymotrypsin-sensitive immunoreactive NHE1 was used to quantify the amount of each one of the mutants expressed at the cell surface.

PIP₂ Content Measurements

Two methods were used to quantify the PIP$_2$ content of AP-1/NHE1$'_{HA}$ cells. Radiolabeled PIP$_2$ was quantified by TLC, essentially as described by Okada et al. (1994). Cells were incubated at 37°C for 1 h in a phosphate-free medium, followed by incubation for 1 h with [^{32}P]orthophosphate (150 μCi/ml). Next, the cells were washed twice with PBS and, where indicated, depletion of cellular ATP was induced. Cells were washed twice more with ice-cold PBS, scraped off the wells with a rubber policeman, and sedimented. For lipid extraction ~10^6 cells were resuspended in 620 μl of chloroform/methanol/8% HClO$_4$ (50:100:5). The mixture was vortexed and 200 μl of chloroform and 200 μl of 8% HClO$_4$ were added to separate the organic phase, which was washed with chloroform-saturated 1% HClO$_4$ before being dried under N$_2$. The dried lipids were dissolved in 15 μl of 95:5 chloroform/methanol to be spotted on a silica gel H plate (Analtech) that had been preactivated by heating at 80°C for 90 min before spotting. The plate was developed in chloroform/acetone/methane/acetic acid/water (80:30:26:24:14) and dried. Radioactivity was quantified with a Molecular Dynamics Storm 840 PhosphorImager.

PIP$_2$ content was also assessed by immunoblotting. Approximately 10^6 AP-1/NHE1$'_{HA}$ cells were washed three times with large volumes of ice-cold PBS, scraped off the wells with a rubber policeman, and sedimented. The cells were resuspended in ~15 vol of methanol/chloroform/concentrated HCl (100:50:1). The mixture was vortexed and 1 vol (equal to the volume of the original cell pellet) of 100 mM EDTA was added. Chloroform (5 vol) and water (5 vol) were added, the cloudy mixture was swirled and centrifuged at 400 g for 5 min to induce phase separation. The bottom (organic) phase was transferred to glass tubes and dried under a stream of N$_2$. The dried lipid extract was redissolved in 10 μl of 1:1 chloroform/methanol (containing 0.1% HCl) and spotted onto polyvinylidene difluoride membranes (Millipore). After drying, blots were blocked overnight at 4°C in TBS containing 3% BSA. Blots were exposed to a 1:500 dilution of mouse mAbs against PIP$_2$. The secondary antibody, goat anti–mouse coupled to HRP, was used at 1:5,000 dilution. Immunoreactive bands were visualized by enhanced chemiluminescence.

Construction and Expression of Glutathione-S-transferase (GST) Fusion Proteins

GST-NHE1 fusion proteins were constructed by amplifying cDNA regions encoding the COOH-terminal amino acids 506–576 of wild-type and mutant (M1, M2, and M1 + 2) NHE1$'_{HA}$ by PCR using the appropriate 5′ and 3′ primers containing unique BamHI and EcoRI restriction sites, respectively, at their 5′-ends. The BamHI-EcoRI DNA fragments were subcloned into the corresponding sites of pGEX-2T and sequenced to confirm the fidelity of the fusion constructs. The plasmid encoding a fusion between GST and residues 548–813 of NHE1 was provided by Dr. L. Fliegel (University of Edmonton, Alberta, Canada). GST fusion proteins were expressed in competent DH5α bacteria and purified using glutathione-agarose as described (Frangioni and Neel, 1993).

PIP₂ Binding Determinations

To assay their ability to bind lipids, GST fusion proteins were allowed to adhere overnight at 4°C onto 96-well plates (1 μg protein in 50 mM sodium bicarbonate buffer, pH 9.6 per well). After washing three times with the sodium bicarbonate buffer, the wells were overlaid for 2 h at room temperature with PIP$_2$ (1 μg/well). After three washes to remove unbound lipid, the samples were blocked with 5% nonfat dried milk and exposed overnight at 4°C to a 1:500 dilution of mouse mAb to PIP$_2$. The secondary antibody, goat anti–mouse coupled to HRP, was used at 1:2,000 dilution in the presence of 2.5% nonfat dried milk. Sigma Fast OPD tablets were used as a substrate for the detection of peroxidase activity. Absorbance at 450 nm was quantified on a microtiter plate reader.

Results

Effect of ATP Depletion on NHE1 Activity and PIP₂ Content

To test the involvement of phosphoinositides in the regulation of NHE1 by ATP, the nucleotide was depleted by incubation for 10 min in a medium containing inhibitors of
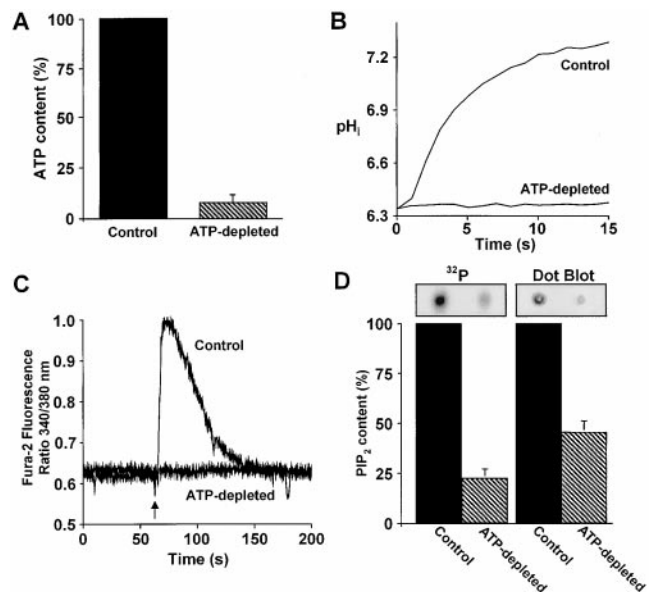

Figure 1. Effect of intracellular ATP depletion on NHE activity and on total PIP$_2$ content. AP-1/NHE1$'_{HA}$ cells were either untreated (Control) or metabolically depleted by incubation with 5 mM 2-deoxy-D-glucose and 5 μg/ml antimycin A for 10 min at 37°C. (A) Intracellular ATP content determined using luciferin–luciferase. Results were normalized to the control and are the mean ± SE of four determinations. (B) Measurement of intracellular pH (pH$_i$) using BCECF. The cells were acid-loaded by prepulsing with NH$_4^+$ and recording was started upon addition of Na$^+$ to the bathing medium. Representative of four similar pH$_i$ determinations. (C) Measurement of cytosolic Ca^{2+} using Fura-2. Where indicated by the arrow, purinergic receptors were activated by addition of 1 mM extracellular ATP. Representative of four similar determinations. (D) Determination of PIP$_2$ content. Lipids were extracted from control or ATP-depleted cells, and the PIP$_2$ content was measured by TLC of ^{32}P-labeled PIP$_2$ (two leftmost bars) or by immunological detection of PIP$_2$ on dot-blots (two rightmost bars) as described in Materials and Methods. The insets show representative experiments, while the main panel summarizes the results of three chromatography and four dot-blot assays, normalized to the control (mean ± SEM).

both glycolysis (2-deoxy-D-glucose) and mitochondrial respiration (antimycin A). As shown in Fig. 1 A, such treatment resulted in the consistent depletion of ≥90% of the cellular ATP. Depletion was performed in K$^+$-rich solution to preclude Na$^+$ loading and dissipation of the inward Na$^+$ gradient, which drives Na$^+$/H$^+$ exchange due to the loss of Na$^+$/K$^+$-ATPase activity. Despite these precautions, depletion of ATP caused a pronounced inhibition of NHE1, in agreement with earlier observations Cassel et al., 1986; Brown et al., 1991; Levine et al., 1993; Kapus et al., 1994; Aharonovitz et al., 1999). The robust Na$^+$-induced recovery from a mild acid load (pH$_i$ ~6.4) observed in untreated cells transfected with NHE1$'_{HA}$ was inhibited by ≥90% after metabolic depletion (Fig. 1 B).

We next analyzed whether metabolic depletion was accompanied by a reduction in the content of cellular PIP$_2$. This phospholipid is the primary substrate of phosphoinositide-specific PLC, which upon activation by agonists, releases diacylglycerol and inositol 1,4,5,-trisphosphate

(IP$_3$). The latter induces the release of calcium stored in the ER, promoting an increase in [Ca^{2+}]$_i$. Depletion of plasmalemmal PIP$_2$, the substrate of the phospholipase, would be expected to blunt the [Ca^{2+}]$_i$ response to agonists. Therefore, we measured [Ca^{2+}]$_i$ in AP-1/NHE1'$_{HA}$ cells subjected to purinergic stimulation. In otherwise untreated cells, purinergic activation led to a rapid and transient elevation in [Ca^{2+}]$_i$ (Fig. 1 C). Because the cells were suspended in Ca^{2+}-free medium, this response reflected exclusive mobilization of intracellular stores by IP$_3$. By comparison, the transient was virtually eliminated in ATP-depleted cells. Failure to respond was not attributable to complete depletion of calcium stored in endomembrane compartments, since addition of ionomycin, a Ca^{2+} ionophore, elicited a sizable [Ca^{2+}]$_i$ increase (not illustrated). These findings are consistent with depletion of PIP$_2$, but other mechanisms may also have contributed to this effect.

The cellular content of PIP$_2$ was analyzed more directly by radiolabeling phospholipids in situ with [^{32}P]orthophosphate, followed by their separation by thin layer chromatography. Using this approach, the amount of ^{32}P-labeled PIP$_2$ decreased by >75% when AP-1/NHE1'$_{HA}$ cells were subjected to the ATP-depletion protocol for 10 min (Fig. 1 D).

Because radiolabeling with [^{32}P]orthophosphate may not have attained equilibrium, it is conceivable that the labeled pool of PIP$_2$ is not representative of the total content of the phosphoinositide. Therefore, the total content of PIP$_2$ was analyzed using a novel immunoblotting assay. Total cellular lipids were extracted in acidified chloroform/methanol, dried, and spotted onto polyvinylidene difluoride. The amount of PIP$_2$ was estimated by blotting with a PIP$_2$-specific antibody, which, in turn, was detected by enhanced chemiluminescence. To validate this novel procedure, we compared the PIP$_2$ content of control and ionomycin-treated cells. By elevating [Ca^{2+}]$_i$, this ionophore is known to activate PLC, thereby reducing the cellular content of PIP$_2$ (Rhee and Bae, 1997). Exposure of the cells to 10 μM ionomycin for 5 min reduced the PIP$_2$ content by 53% (not shown). As shown in Fig. 1 D, depletion of ATP similarly reduced the PIP$_2$ content by >50%, consistent with the chromatographic data.

Effect of ATP Depletion on Plasmalemmal PIP$_2$ Content

Regardless of the method used for PIP$_2$ determination, depletion of the phosphoinositide in metabolically inhibited cells was incomplete after 10 min. This may reflect the existence of multiple subcellular pools of PIP$_2$ with varying susceptibility to ATP depletion. Because NHE1 is likely to be affected exclusively by plasmalemmal PIP$_2$, we sought methods to analyze this subcompartment more specifically. To this end, we took advantage of the recent observation that the PH domain of PLCδ binds with high affinity and selectivity to PIP$_2$ (Ferguson et al., 1995; Lemmon et al., 1995). Therefore, we constructed a cDNA encoding a chimeric protein encompassing this PH domain and enhanced GFP (PH$_{PLCδ}$-GFP), to monitor the subcellular distribution of PIP$_2$ before and after depletion of ATP. As reported for other cell types (Stauffer et al., 1998; Varnai and Balla, 1998), the chimeric protein is largely associated

with the plasma membrane of otherwise untreated AP-1/NHE1'$_{HA}$ cells (Fig. 2 A). Activation of PLC by addition of ionomycin induced the rapid translocation of PH$_{PLCδ}$-GFP to the cytosol, an indication of PIP$_2$ hydrolysis (Fig. 2 B), as reported previously (Varnai and Balla, 1998). Similarly, the chimeric protein was displaced from the membrane by incubation with neomycin (Fig. 2 C), a cell-permeant cationic antibiotic known to bind tightly to the headgroup of phosphoinositides (Schacht, 1976). Importantly, ATP depletion also resulted in extensive translocation of PH$_{PLCδ}$-GFP from the membrane to the cytosol (Fig. 2 D). The displacement was almost complete, comparable in extent to that induced by ionomycin and neomycin (Fig. 2 E). Jointly, these results indicate that the meta-
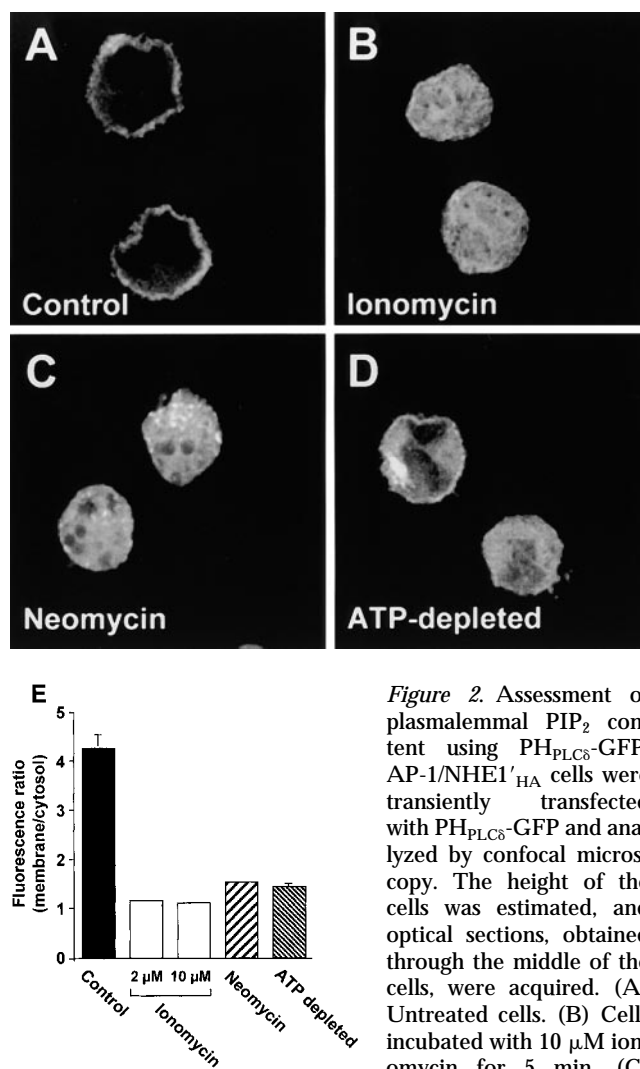

Figure 2. Assessment of plasmalemmal PIP$_2$ content using PH$_{PLCδ}$-GFP. AP-1/NHE1'$_{HA}$ cells were transiently transfected with PH$_{PLCδ}$-GFP and analyzed by confocal microscopy. The height of the cells was estimated, and optical sections, obtained through the middle of the cells, were acquired. (A) Untreated cells. (B) Cells incubated with 10 μM ionomycin for 5 min. (C) Cells preincubated overnight with 5 mM neomycin. (D) Cells that were ATP depleted as in Fig. 1. Images shown in A–D are representative of four independent experiments. (E) Ratio of the fluorescence intensity determined at the outermost edge of the image (plasma membrane or outermost layer of the cytosol) divided by the fluorescence of an equivalent area measured near the center of the cell (cytosol). Data are means ± SEM of at least 20 determinations of each kind, from four similar experiments. Where absent, error bars are smaller than the lines limiting the bars.
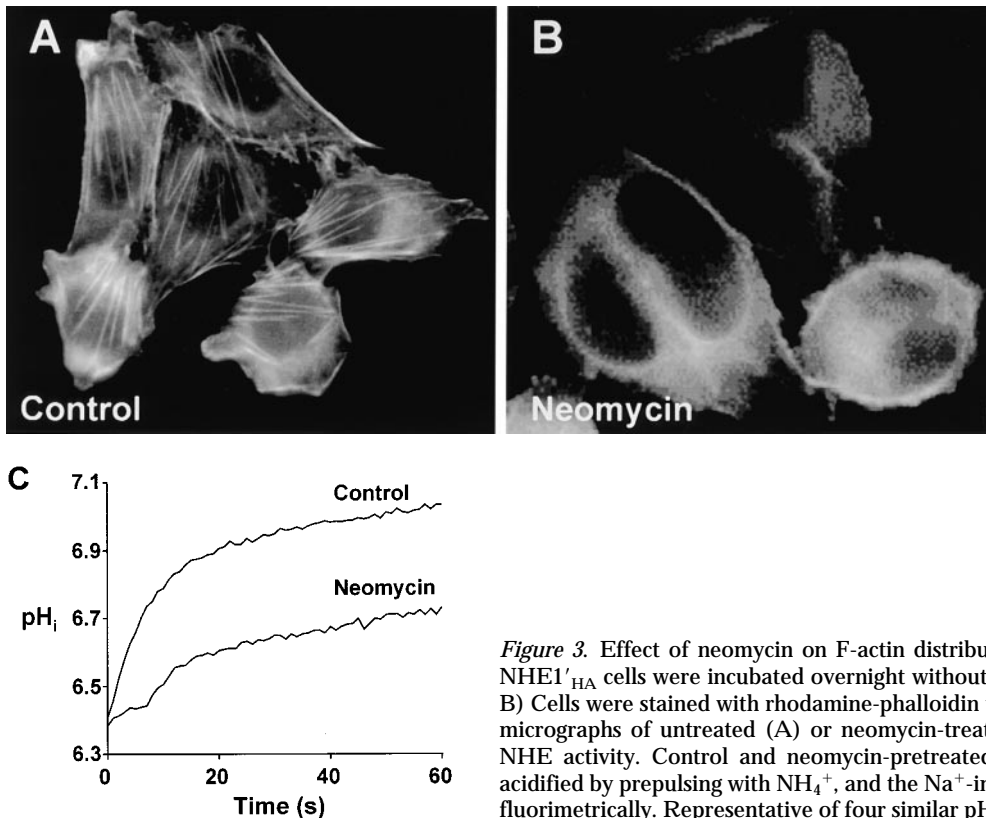
Figure 3. Effect of neomycin on F-actin distribution and on NHE1 activity. AP-1/NHE1'$_{HA}$ cells were incubated overnight without or with neomycin (5 mM). (A and B) Cells were stained with rhodamine-phalloidin to visualize F-actin. Representative micrographs of untreated (A) or neomycin-treated (B) cells. (C) Measurement of NHE activity. Control and neomycin-pretreated cells were loaded with BCECF, acidified by prepulsing with NH_4^+, and the Na^+-induced alkalinization was measured fluorimetrically. Representative of four similar pH$_i$ determinations.

bolic depletion protocol used for inhibition of NHE1 concomitantly causes depletion of plasmalemmal PIP$_2$.

Effect of Neomycin on NHE1 Activity

The correlation between the depletion of ATP and the reduction in PIP$_2$ content suggests, but does not prove, that binding of the phosphoinositide to NHE1 modulates the rate of Na$^+$/H$^+$ exchange. To further evaluate this hypothesis, we sought to modify the amount of available PIP$_2$ without simultaneously depleting the intracellular ATP.

Neomycin has been shown to bind tightly to PIP$_2$, restricting the availability of its headgroup to proteins including PLC (Downes and Michell, 1981). Therefore, we tested whether neomycin would similarly interfere with the putative interaction between NHE1 and PIP$_2$. Cells expressing wild-type NHE1 were preincubated with neomycin to allow entry of the antibiotic and sequestration of PIP$_2$. As shown above, this resulted in effective displacement of PH$_{PLC\delta}$-GFP from the inner surface of the plasma membrane (Fig. 2, compare A and C). Because several actin-binding proteins are modulated by PIP$_2$ (Yu et al., 1992), we also evaluated the effects of neomycin in cells stained with rhodamine-phalloidin. As illustrated in Fig. 3, the stress fibers, which are routinely observable in AP-1/NHE1 cells, were largely eliminated by treatment with neomycin. The antibiotic also increased the number of binucleated cells (Fig. 3 B), a phenotype that was associated earlier with hydrolysis of PIP$_2$ by synaptojanin (Sakisaka et al., 1997). These observations suggest that neomycin effectively entered the cells, where it interacted with the headgroup of PIP$_2$. Fig. 3 C illustrates the effect of neomy-

cin on NHE1 activity. On average, the antibiotic depressed the initial rate of recovery from an acid load by 62% ($n = 4$). These observations are consistent with the notion that PIP$_2$ regulates the activity of NHE1.

Effect of Calcium-induced PIP$_2$ Depletion

Elevation of [Ca^{2+}]$_i$ can activate endogenous PLC, thereby inducing hydrolysis of PIP$_2$. The effectiveness of this maneuver was documented earlier in cells transfected with PH$_{PLC\delta}$-GFP (Fig. 2). Therefore, we used this approach as an alternative means of decreasing the content of plasmalemmal PIP$_2$, to assess its effects on NHE1. However, it is noteworthy that calcium can also alter the activity of NHE1 by mechanisms that do not involve PIP$_2$. Specifically, NHE1 possesses sites that interact with calcium–calmodulin, resulting in stimulation of antiport activity (Bertrand et al., 1994). Therefore, it was important to dissociate the direct effects of calcium on the exchanger from its indirect action mediated by PLC. This was accomplished by using cells transfected with NHE1Δ582, a truncated form of the exchanger that lacks the calmodulin-binding sites (residues 636–656 and 657–700).

As shown in Fig. 4 A, this truncated version of NHE1 actively exchanges Na$^+$ for H$^+$ and, more importantly, displays marked sensitivity to ATP. In five experiments, the rate of pH recovery in NHE1Δ582 transfectants, measured at pH$_i$ 6.4, was inhibited by 87% (Fig. 4 B) upon metabolic depletion. Next, we tested the effects of ionomycin on H$^+$ extrusion. The contribution of Ca^{2+}/H$^+$ exchange mediated by the ionophore to the rate of pH$_i$ change was minimized by measuring the pH$_i$ recovery in a Ca^{2+}-free me-
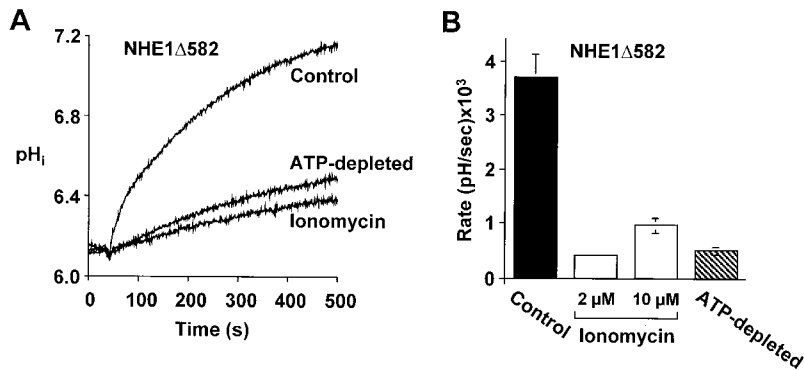
Figure 4. Effects of ATP depletion and of iono-mycin on the exchange activity of NHE1Δ582. AP-1 cells stably transfected with NHE1Δ582 were either untreated (Control), ATP depleted as in Fig. 1, or incubated with either 2 or 10 μM ionomycin for 5 min. Acid loading and fluorimetric determination of pH_i were as in Fig. 3. Note that ATP depletion and treatment with ionomycin were performed during the final stages of BCECF loading. (A) Representative pH_i determinations. (B) Rates of recovery measured at pH_i 6.4 are summarized as means ± SEM of at least four determinations.

dium. Treatment with either 2 or 10 μM ionomycin greatly inhibited NHE1 activity (Fig. 4, A and B). Importantly, we ascertained that treatment with the Ca^{2+} ionophore did not affect the cellular ATP content (e.g., in cells treated with 2 μM ionomycin ATP was 93% of the control). Together with the neomycin experiments, these results indicate that conditions that block or deplete plasmalemmal PIP_2 markedly inhibit the activity of NHE1.

Effect of Overexpression of PIP_2-binding PH Domains on NHE Activity

As described above, the PH domain of $PH_{PLC\delta}$, which binds preferentially to the headgroup of PIP_2, can be used to detect the location of the phosphoinositide. If expressed in large quantity, however, $PH_{PLC\delta}$ will effectively compete with endogenous ligands for binding to the finite amount of plasmalemmal PIP_2. To assess the dependence of NHE1 activity on PIP_2, we expressed $PH_{PLC\delta}$-GFP in COS-1 cells. These cells express the T antigen and, therefore, allow the replication of vectors containing the SV40 origin, with consequent amplification of the amount of protein expressed. The presence of the SV40 origin of replication in the pEGFP vector enabled us to test the effect of overexpression of $PH_{PLC\delta}$-GFP on NHE activity in COS-1 cells. The results of these experiments are illustrated in Fig. 5. Sequestration of PIP_2 by $PH_{PLC\delta}$-GFP greatly reduced the rate of Na^+-induced pH recovery in acid-loaded cells (Fig. 5 A). In five separate experiments, the initial rate of alkalinization was inhibited by ≥80% (Fig. 5 B).

Effect of a PIP_2 Phosphatase on NHE Activity

The putative role of PIP_2 in regulating NHE1 was also tested using a 5′-specific PIP_2 phosphatase. To selectively reduce plasmalemmal PIP_2, cells were transfected with a yeast 5′-specific phosphatase, Inp54p, targeted to the plasma membrane by fusion with a myristoylation/palmitoylation sequence from the NH_2 terminus of Lyn (Raucher et al., 2000). GFP was also included in this chimeric construct, termed PM-5′-phosphatase-GFP, to facilitate identification of the transfected cells. Inp54p was shown recently to function as an effective 5′-phosphatase towards PIP_2 both in vitro and in vivo (Raucher et al., 2000). When expressed in COS-1 cells, PM-5′-phosphatase-GFP markedly inhibited Na^+/H^+ exchange (Fig. 5 B). The accumulated evidence strongly suggests that nor-

mal levels of plasmalemmal PIP_2 are essential for optimal NHE1 function.

Binding of PIP_2 to NHE1

The mechanism underlying the inhibition of NHE activity upon depletion of plasmalemmal PIP_2 was investigated next. As suggested for other transporters (Huang et al., 1998), it is conceivable that PIP_2 binds directly to the exchanger, thereby modulating its activity. Indeed, perusal of the primary structure of NHE1 revealed the presence of two sequences that resemble the PIP_2-binding motifs of a variety of proteins, including gelsolin and profilin (Yu et al., 1992). These putative PIP_2-binding motifs (residues 513–520, called hereafter site 1, and 556–564, site 2) are located in the cytosolic tail, near the predicted point of emergence of the last putative transmembrane domain (residue 504). The sequences of these motifs, which alternate cationic and hydrophobic residues and a schematic
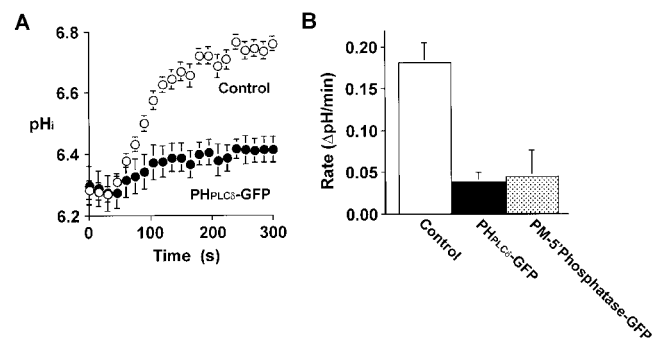

Figure 5. Effects of $PH_{PLC\delta}$-GFP and PM-5′-phosphatase-GFP on NHE activity. COS-1 cells were transiently transfected with either $PH_{PLC\delta}$-GFP or PM-5′-phosphatase-GFP. After 24 h, transfected cells were identified by visualizing GFP fluorescence. A neutral density filter was interposed in the light path, and the cells were stained with BCECF while on the microscope stage. Acid loading and fluorimetric determination of pH_i were as in Fig. 3. (A) Fluorimetric pH_i determinations in control (open circles) and $PH_{PLC\delta}$-GFP–transfected cells (solid circles). Na^+ was added after 45 s. Values are means ± SEM of at least five determinations. (B) Rates of pH_i recovery measured during the first minute after the addition of Na^+ in experiments like that in A are summarized as means ± SEM for control ($n = 21$), $PH_{PLC\delta}$-GFP ($n = 5$), or PM-5′-phosphatase-GFP ($n = 3$)–transfected cells.
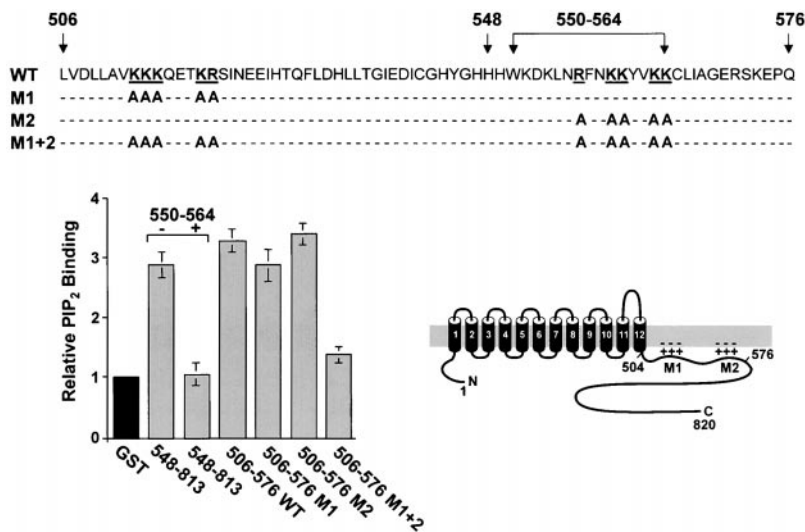
Figure 6. Binding of PIP$_2$ to NHE1-derived fusion proteins. (Top) Primary sequence of the juxtamembrane region of NHE1 (residues 506–576) that contains two potential PIP$_2$-binding domains. The wild-type (WT) sequence is shown at the top, highlighting the cationic residues within the putative PIP$_2$-binding sites 1 and 2. The synthetic peptide, which is used for competition experiments (residues 550–564), is bracketed. In mutant 1 (M1), the cationic residues in site 1 were mutated to alanine (second line). In mutant 2 (M2), the cationic residues in site 2 were mutated to alanine (third line). In the double mutant (M1 + 2), both sets of cationic residues were mutated (bottom line). (bottom left) Graph showing results of PIP$_2$ binding determinations to either GST alone (leftmost bar) or GST fusions encompassing the indicated regions of NHE1. Where specified, sites 1 and/or 2 were mutated as above. Where indicated, peptide 550–564 was added to compete for PIP$_2$ binding. Results are normalized to the binding to GST, and are means ± SEM of eight determinations. (bottom right) Schematic representation of the predicted topology of NHE1, indicating the location of the putative PIP$_2$-binding sites 1 and 2.

representation of their location within the predicted topology of NHE1, are illustrated in Fig. 6.

Recombinant fusion proteins and synthetic peptides encompassing one or both of these motifs were generated to test their ability to interact with PIP$_2$. A summary of the results is presented in the Fig. 6 (bottom left). In brief, a fusion of GST with residues 548–813 bound PIP$_2$ with much greater efficiency than GST alone (such excess binding is defined hereafter as "specific binding"). This suggests that residues encompassing the site 2 motif may be involved in phosphoinositide binding. Accordingly, preincubation of the lipid with a synthetic 550–564 peptide precluded specific binding of PIP$_2$ to the GST (548–813) fusion protein. To more precisely evaluate the role of the juxtamembrane domain of NHE1 in PIP$_2$ binding, we analyzed GST fusions encompassing residues 506–576 and several mutants where the cationic residues were simultaneously replaced by alanine. As shown in Fig. 6, GST-NHE1(506–576) bound PIP$_2$ to an extent comparable to that found for the 548–813 construct. Elimination of the NH$_2$-terminal cationic motif (^{513}KKKQETKR^{520} to ^{513}AAAQETAA^{520}; residues involved in mutagenesis are underlined; M1 mutant in Fig. 6) had little effect on phosphoinositide binding. Unexpectedly, mutation of the more COOH-terminal motif (^{556}RFNKKYVKK^{564} to ^{556}AFNAAYVAA^{564}; M2 mutant in Fig. 6) was equally ineffectual. However the combined mutation of both motifs (Fig. 6, M1 + 2) largely eliminated specific PIP$_2$ binding. These findings suggest that either motif is capable of binding the phospholipid, and that only one site can be occupied at any one time. Because of the comparatively large size of PIP$_2$ micelles (∼90 kD), binding of one such micelle to either motif likely precludes binding of a second one to the other cationic sequence. Indeed, both sites may interact with the same micelle simultaneously.

Mutation of Putative PIP$_2$-binding Motifs: Functional Consequences

Having identified two PIP$_2$-binding motifs in the cytosolic domain of NHE1, we proceeded to assess their functional role. Stable lines were generated by transfecting antiport-deficient AP-1 cells with either full-length wild-type NHE1, or with mutated forms containing substitutions of the cationic residues in either one or both putative PIP$_2$-binding motifs with alanines, identical to those engineered in the GST-NHE1(506–576) fusions. All constructs were epitope-tagged to facilitate their immunological detection. As illustrated in Fig. 7 A, the two singly mutated constructs of NHE1 (also called M1 and M2, by analogy with Fig. 6), as well as the double mutant (M1 + 2) generated full-length proteins that were at least partly expressed at the plasma membrane. Two lines of evidence indicate that the mutant proteins reach the plasma membrane. First, transfected AP-1 cell lines were selected by their ability to survive an acid challenge, indicating that the mutant exchangers were functional and, therefore, most likely at the cell surface. Second, as found earlier for wild-type NHE1 (Shrode et al., 1998), two distinct species of the mutant proteins were detected by immunoblotting: a faster migrating band that approximates the molecular mass predicted from the primary sequence, and a form that is larger and more heterogeneous as a result of complex glycosylation (Fig. 7 A). In the case of wild-type NHE1, the former was shown to be an immature intracellular species, whereas the fully glycosylated form reaches the plasma membrane. The similarity in the expression patterns suggests that the mutants are also fractionally targeted to the surface membrane. More direct evidence was obtained from analyzing the susceptibility of the proteins to chymotrypsin. When added to the external medium, this protease cleaves the glycosylated wild-type NHE1, yielding a membrane-bound form of increased mobility that lacks carbohydrate (Shrode et al., 1998). By contrast, the intracellular species is refractory to the protease, as anticipated. An identical proteolysis pattern was observed for the three mutant forms of NHE1, implying that they are properly processed and inserted in the plasma membrane.
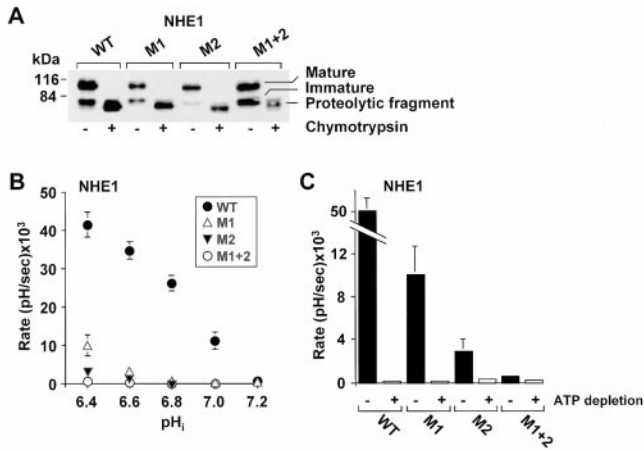
Figure 7. Comparative analysis of Na$^+$-induced pH$_i$ recovery of AP-1 cells transfected with wild-type and mutant forms of NHE1 under control and ATP-depleted conditions. (A) Analysis of surface expression of NHE1$'_{HA}$ by immunoblotting. AP-1 cells were stably transfected with wild-type or mutant (M1, M2, and M1 + 2) NHE1$'_{HA}$. The cells were treated with or without chymotrypsin (100 U/ml, 5 min) and whole cell extracts were analyzed by electrophoresis and immunoblotting with anti-HA antibody. Note that the amounts of protein loaded are not identical: NHE1 = 4 µg; NHE1-M1 = 4 µg; NHE1-M2 = 10 µg; and NHE1-M1 + 2 = 7 µg. The position of the fully glycosylated (∼105 kD, Mature) and incompletely glycosylated (∼80 kD, Immature) forms of full-length NHE1, and of the main proteolytic fragment (∼75 kD) are shown. The blot is representative of three similar experiments. (B) Comparison of the Na$^+$/H$^+$ exchange activity determined from the rate of H$^+$ extrusion as in Fig. 3 in AP-1 cells transfected with wild-type or mutant forms of NHE1$'_{HA}$. The rates of Na$^+$-induced alkalinization were recorded, normalized for plasmalemmal NHE1 expression, and displayed as a function of the pH$_i$. Data are means ± SEM of at least five determinations. Where absent, error bars are smaller than the symbol. (C) AP-1 cells transfected with wild-type or mutant forms of NHE1$'_{HA}$ were either untreated or subjected to ATP depletion, as in Fig. 1. The rates of Na$^+$-induced alkalinization measured at pH$_i$ 6.4 are illustrated. Data are means ± SEM of at least four determinations.

Having ascertained that the mutants were appropriately expressed and targeted, we proceeded to evaluate the effect of the mutations on the basal rate of transport and on the ATP dependence of this process. The expression level of the exchangers varied among the transfected lines, and meaningful comparison of their rates of transport required normalization with respect to the number of plasmalemmal exchangers. This was estimated from the relative intensities of the chymotrypsin-sensitive bands in immunoblots, as shown in Fig. 7 A. Using this procedure, we compared the rates of Na$^+$/H$^+$ exchange in acid-loaded wild-type and mutant cells by measuring the pH$_i$ recovery induced by Na$^+$. It is noteworthy that in all cases, the rate of alkalinization was negligible in the absence of Na$^+$ (data not shown). A comparison of the basal rates of transport is shown in Fig. 7 B. Mutation of the juxtamembrane cationic residues (mutant M1) drastically reduced the efficiency of transport. At a pH$_i$ of 6.4, exchange was inhibited by ∼80%. An even greater inhibition was noted when the more COOH-terminal cationic cluster was mutated

(mutant M2), and transport was negligible when both mutations were present simultaneously (mutant M1 + 2). A similar pattern was noted when NHE activity was assessed independently by measuring ^{22}Na$^+$ influx in cells clamped at different pH$_i$ ranging from 5.4 to 7.4 (Fig. 8, A–D). In these experiments, the radioisotope uptake at pH$_i$ 5.4, when normalized for cell-surface NHE1$'_{HA}$ protein expression, was decreased by 78, 90, and 94% in M1, M2, and M1 + 2 cells, respectively, compared with wild-type NHE1$'_{HA}$. These results indicate that the motifs capable of binding PIP$_2$ are essential for optimal Na$^+$/H$^+$ exchange by NHE1.

We next compared the effect of ATP depletion on the activity of the wild-type and mutated forms of NHE1. As shown earlier, metabolic depletion induced a marked depression in the rate of Na$^+$/H$^+$ exchange by native NHE1$'_{HA}$, measured either as pH$_i$ recovery from a mild acid load (pH$_i$ 6.4; Fig. 7 C) or as ^{22}Na$^+$ influx over a broader pH$_i$ range (Fig. 8 A). With respect to ^{22}Na$^+$ influx, the inhibition was most noticeable at pH$_i$ 6.6, but was partially relieved at more acidic pH$_i$ levels (i.e., activity restored to 70–80% of wild-type values at pH$_i$ 5.4), in agreement with an earlier report (Ikeda et al., 1997). Despite their comparatively low rates of transport in the presence of ATP, the M1 and M2 mutants were further inhibited by
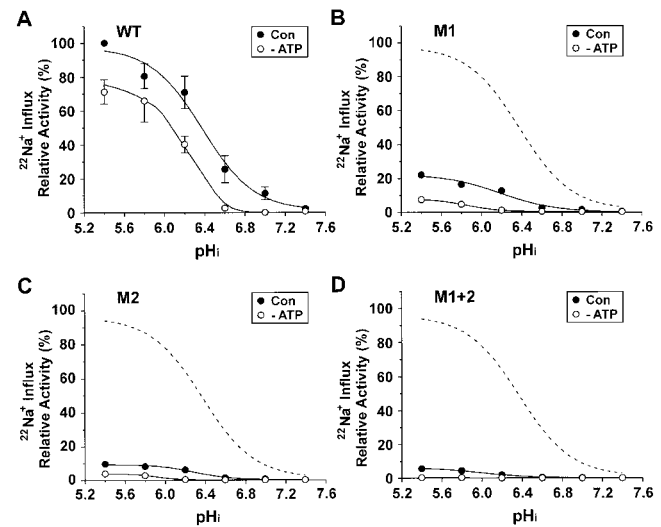

Figure 8. Comparative analysis of rates of ^{22}Na$^+$ influx of AP-1 cells transfected with wild-type and mutant forms of NHE1 under control and ATP-depleted conditions. AP-1 cells transfected with wild-type (WT) or mutant forms (M1, M2, and M1 + 2) of NHE1$'_{HA}$ were either untreated (Con) or subjected to ATP depletion (−ATP). (A–D) The cells were clamped at the indicated pH$_i$, and the rates of ^{22}Na$^+$ uptake were measured, as detailed in Material and Methods. (A) WT; (B) M1; (C) M2; and (D) M1 + 2. To facilitate comparison of the effects of mutating the PIP$_2$-binding sites, the rates of ^{22}Na$^+$ influx of wild-type and the mutant forms of NHE1 were normalized to their respective plasmalemmal protein levels, and then expressed relative to the maximal uptake rate of wild-type NHE1. In B–D, the dashed line indicates the wild-type NHE1 profile in control cells. Data are means ± SEM of three separate experiments, each performed in quadruplicate. Where absent, error bars are smaller than the symbol.

depletion of the nucleotide (Fig. 7 C, and Fig. 8, B and C). At pH_i 6.4, the basal rate of transport in the dual mutant M1 + 2 was so low that no significant diminution could be detected after ATP depletion by measurements of pH_i (Fig. 7 C). However, using the more sensitive isotopic method (Fig. 8 D), the small, residual activity measurable in the double mutant retained some sensitivity to metabolic depletion. Unlike the flux in wild-type cells, however, the inhibition caused by ATP depletion could not be reversed by lowering the pH_i. These findings suggest that ATP depletion exerts a dual effect on NHE1: one component of the inhibitory response is mimicked by elimination of the phosphoinositide-binding sites 1 and 2 and can be counteracted by lowering pH_i, whereas a second, smaller component is independent of sites 1 and 2, and is not reversed by acidification.

Discussion

Binding of PIP₂ to NHE1

It is well established that PIP_2 plays a central role in signal transduction as a precursor to IP_3 and diacylglycerol (Rhee and Bae, 1997). However, it was only recently appreciated that PIP_2 is essential for the regulation of several processes by acting as a direct ligand or cofactor of a variety of proteins. Physical interaction of PIP_2 with proteins containing specific PH domains serves to target them to the vicinity of their substrates (Lemmon et al., 1997). Moreover, association with PIP_2 can promote assembly of cytoskeletal proteins (Sakisaka et al., 1997), and alters the functional activity of enzymes and transporters (Hilgemann and Ball, 1996; Baukrowitz et al., 1998; Huang et al., 1998). NHE1 can now be added to the growing list of proteins that bind to, and are regulated by, PIP_2. The evidence supporting this contention is as follows. First, the COOH-terminal domain of NHE1 includes two sequences that resemble PIP_2-binding motifs identified in other proteins. Second, the recombinant COOH terminus of NHE1 can bind PIP_2 in vitro and a synthetic peptide containing one of the putative PIP_2-interacting motifs effectively competes for such binding. Third, mutation of the cationic residues within the putative PIP_2-binding motifs has profound effects on the activity of NHE1. Fourth, sequestration of PIP_2 with neomycin or $PH_{PLC\delta}$-GFP reduced NHE activity; and fifth, depletion of PIP_2 with ionomycin or PM-5′ phosphatase induced a marked inhibition of NHE1.

Mutation of either site 1 or 2 greatly depressed ion exchange (Figs. 7 and 8), whereas elimination of both sites was required to eliminate PIP_2 binding (Fig. 6). This apparent discrepancy can be readily explained by assuming that, while both sites 1 and 2 can bind PIP_2 separately, simultaneous binding at both sites is required for optimal transport. Indeed, the in vitro findings suggest that either motif is capable of binding the phospholipid. Because of the large size of the PIP_2 micelle, it is likely that only one micelle can bind to each fusion protein. This explains why binding is not greater when the protein has two cationic domains than when it contains only one.

The mechanism whereby PIP_2 alters the activity of the exchanger remains to be defined. In the case of the Na^+/Ca^{2+} exchanger, an analogous PIP_2-binding motif is thought to be autoinhibitory, since cytosolic perfusion with a synthetic peptide of similar sequence antagonizes exchange (DiPolo and Beauge, 1994). Binding of the motif to PIP_2 is believed to sequester it away from the transport moiety of the protein, precluding its autoinhibitory effect (Shannon et al., 1994). In principle, a similar mechanism could be envisaged for NHE1. However, deletion and truncation experiments are inconsistent with this model. Unlike the Na^+/Ca^{2+} exchanger, which remains functional after removal of the PIP_2-binding motif, NHE1 becomes greatly inhibited when the region encompassing sites 1 and 2 is truncated (Ikeda et al., 1997; Orlowski, J., and S. Grinstein, unpublished observations) or mutated (Figs. 7 and 8). We feel it is more likely, instead, that the optimal transport configuration of NHE1 requires the tight apposition of sites 1 and/or 2 with the inner surface of the plasma membrane. Departures from this configuration, induced either by truncation, mutation, or depletion of the PIP_2 required to maintain the protein in place, result in inhibition of transport.

While we have shown that NHE1 can interact with PIP_2 in vitro, the existence of such an interaction in situ remains inferential, based exclusively on the functional effects of phosphoinositide depletion. It is therefore possible that such functional effects may be indirect. In this regard, it is noteworthy that ezrin was recently reported to interact with NHE1 (Denker et al., 1998). Members of the ezrin/radixin/moesin (ERM) family are themselves capable of binding PIP_2, which in turn modulates the ability of ERM to interact with other proteins (Hirao et al., 1996). Therefore, one could envisage a model wherein the availability of PIP_2 dictates the extent of association of ERM proteins with NHE1. The latter interaction may be responsible for modulation of NHE1 activity, though this premise has not yet been tested experimentally. This model would be compatible with most of our observations, but would not account for the observed direct binding of PIP_2 to sites 1 and 2 of NHE1. Finally, it is conceivable that PIP_3 rather than PIP_2 is required for NHE activity, and that the effects of depletion of the latter are indirect. This appears unlikely, in that inhibition of phosphatidylinositol 3′-kinase with wortmannin has no effect on NHE1 activity.

Role of PIP₂ in the ATP Sensitivity of NHE1

The exquisite dependence on PIP_2 could account, at least in part, for the well established ATP sensitivity of NHE1. Several lines of evidence support this notion. First, metabolic depletion is accompanied by a parallel decrease in the total (Fig. 1) and particularly in the plasmalemmal content of PIP_2 (Fig. 2). Second, the extent of NHE inhibition induced by depletion of ATP is comparable to that obtained by extensive hydrolysis of PIP_2 (Fig. 4); and third, elimination of the putative PIP_2-binding motifs greatly reduces the magnitude of the ATP-dependent component of exchange (Figs. 7 and 8). It is also noteworthy that the PIP_2-binding sequences identified in this report are within the region mapped earlier to confer ATP dependence to NHE1 (Ikeda et al., 1997). The hypothesis that PIP_2 mediates the effects of ATP would explain why changes in the phosphorylation of NHE1 itself were not found to correlate with its inhibition in metabolically depleted cells

(Goss et al., 1994) and why mutants such as NHE1Δ582, which lack the phosphorylation sites identified in NHE1, retain their sensitivity to ATP.

While mutation of the putative PIP_2-binding sites 1 and 2 profoundly reduced the ATP-sensitive fraction of Na^+/H^+ exchange, a measurable nucleotide-sensitive component of transport remained (Fig. 8). This implies that an additional, phosphoinositide-independent mechanism contributes to the effect of ATP on NHE1. The existence of two or more sites of action of ATP in the regulation of NHE was suggested previously by the findings of Demaurex et al. (1997), who found that nonhydrolyzable analogues of ATP could partially restore NHE activity in ATP-depleted cells. The target of such nonhydrolyzable nucleotides, which are unable to phosphorylate phosphoinositides, remains undefined. Finally, though the ubiquitous isoform NHE1 was used in this study, the interaction with PIP_2 may extend to other isoforms. Not only are all isoforms, thus far, tested exquisitely sensitive to depletion of ATP, but motifs similar to those postulated to bind PIP_2 in NHE1 exist also in NHE2-5. This conservation of sequence argues in favor of an important role for these motifs in the regulation of Na^+/H^+ exchange.

References

Aharonovitz, O., and S. Grinstein. 1999. Na^+/H^+ exchangers: structure, function and regulation. *Drugs News Perspect.* 12:105–109.

Aharonovitz, O., N. Demaurex, M. Woodside, and S. Grinstein. 1999. ATP dependence is not an intrinsic property of Na^+/H^+ exchanger NHE1: requirement for an ancillary factor. *Am. J. Physiol.* 276:C1303–C1311.

Baukrowitz, T., U. Schulte, D. Oliver, S. Herlitze, T. Krauter, S.J. Tucker, J.P. Ruppersberg, and B. Fakler. 1998. PIP_2 and PIP as determinants for ATP inhibition of K_{ATP} channels. *Science.* 282:1141–1144.

Bertrand, B., S. Wakabayashi, T. Ikeda, J. Pouyssegur, and M. Shigekawa. 1994. The Na^+/H^+ exchanger isoform 1 (NHE1) is a novel member of the calmodulin-binding proteins. Identification and characterization of calmodulin-binding sites. *J. Biol. Chem.* 269:13703–13709.

Brown, S.E., T.A. Heming, C.R. Benedict, and A. Bidani. 1991. ATP-sensitive Na^+-H^+ antiport in type II alveolar epithelial cells. *Am. J. Physiol.* 261:C954–C963.

Cabado, A.G., F.H. Yu, A. Kapus, G. Lukacs, S. Grinstein, and J. Orlowski. 1996. Distinct structural domains confer cAMP sensitivity and ATP dependence to the Na^+/H^+ exchanger NHE3 isoform. *J. Biol. Chem.* 271:3590–3599.

Cassel, D., M. Katz, and M. Rotman. 1986. Depletion of cellular ATP inhibits Na^+/H^+ antiport in cultured human cells. Modulation of the regulatory effect of intracellular protons on the antiporter activity. *J. Biol. Chem.* 261:5460–5466.

Chen, C.A., and H. Okayama. 1988. Calcium phosphate-mediated gene transfer: a highly efficient transfection system for stably transforming cells with plasmid DNA. *Biotechniques.* 6:632–638.

Demaurex, N., R.R. Romanek, J. Orlowski, and S. Grinstein. 1997. ATP dependence of Na^+/H^+ exchange. Nucleotide specificity and assessment of the role of phospholipids. *J. Gen. Physiol.* 109:117–128.

Denker, S., T. Tominaga, and D.L. Barber. 1998. NHE1 links actin cytoskeleton to the plasma membrane by directly interacting with ERM proteins. *Mol. Biol. Cell.* 9:A762.

DiPolo, R., and L. Beauge. 1994. Cardiac sarcolemmal Na/Ca-inhibiting peptides XIP and FMRF-amide also inhibit Na/Ca exchange in squid axons. *Am. J. Physiol.* 267:C307–C311.

Downes, C.P., and R.H. Michell. 1981. The polyphosphoinositide phosphodiesterase of erythrocyte membranes. *Biochem. J.* 198:133–140.

Ferguson, K.M., M.A. Lemmon, J. Schlessinger, and P.B. Sigler. 1995. Structure of the high affinity complex of inositol trisphosphate with a phospholipase C pleckstrin homology domain. *Cell.* 83:1037–1046.

Frangioni, J.V., and B.G. Neel. 1993. Solubilization and purification of enzymatically active glutathione S-transferase (pGEX) fusion proteins. *Anal. Biochem.* 210:179–187.

Gan, B.S., E. Krump, L. Shrode, and S. Grinstein. 1998. Loading pyranine via purinergic receptors or hypotonic stress for measurements of cytosolic pH by imaging. *Am. J. Physiol.* 275:C1158–C1166.

Goss, G.G., M. Woodside, S. Wakabayashi, J. Pouyssegur, T. Waddell, G.P. Downey, and S. Grinstein. 1994. ATP dependence of NHE-1, the ubiquitous isoform of the Na^+/H^+ antiporter. Analysis of phosphorylation and subcellular localization. *J. Biol. Chem.* 269:8741–8748.

Grinstein, S., M. Woodside, C. Sardet, J. Pouyssegur, and D. Rotin. 1992. Activation of the Na/H antiporter during cell volume regulation. Evidence for a phosphorylation-independent mechanism. *J. Biol. Chem.* 267:23823–23828.

Hilgemann, D.W., and R. Ball. 1996. Regulation of cardiac Na^+,Ca^{2+} exchange and K_{ATP} potassium channels by PIP_2. *Science.* 273:956–959.

Hirao, M., N. Sato, T. Kondo, S. Yonemura, M. Monden, T. Sasaki, Y. Takai, S. Tsukita, and S. Tsukita. 1996. Regulation mechanism of ERM (ezrin/radixin/moesin) protein/plasma membrane association: possible involvement of phosphatidylinositol turnover and Rho-dependent signaling pathway. *J. Cell. Biol.* 135:37–51.

Huang, C.L., S. Feng, and D.W. Hilgemann. 1998. Direct activation of inward rectifier potassium channels by PIP_2 and its stabilization by Gβγ. *Nature.* 391:803–806.

Ikeda, T., B. Schmitt, J. Pouyssegur, S. Wakabayashi, and M. Shigekawa. 1997. Identification of cytoplasmic subdomains that control pH-sensing of the Na^+/H^+ exchanger (NHE1): pH-maintenance, ATP-sensitive, and flexible loop domains. *J. Biochem.* 121:295–303.

Kapus, A., S. Grinstein, S. Wasan, R. Kandasamy, and J. Orlowski. 1994. Functional characterization of three isoforms of the Na^+/H^+ exchanger stably expressed in chinese hamster ovary cells. ATP dependence, osmotic sensitivity, and role in cell proliferation. *J. Biol. Chem.* 269:23544–23552.

Kinsella, J.L., and P.S. Aronson. 1980. Properties of the Na^+-H^+ exchanger in renal microvillus membrane vesicles. *Am. J. Physiol.* 238:F461–F469.

Lemmon, M.A., M. Falasca, K.M. Ferguson, and J. Schlessinger. 1997. Regulatory recruitment of signalling molecules to the call membrane by pleckstrin-homology domains. *Trends Cell Biol.* 7:237–242.

Lemmon, M.A., K.M. Ferguson, R. O'Brien, P.B. Sigler, and J. Schlessinger. 1995. Specific and high-affinity binding of inositol phosphates to an isolated pleckstrin homology domain. *Proc. Natl. Acad. Sci. USA.* 92:10472–10476.

Levine, S.A., M.H. Montrose, C.M. Tse, and M. Donowitz. 1993. Kinetics and regulation of three cloned mammalian Na^+/H^+ exchangers stably expressed in a fibroblast cell line. *J. Biol. Chem.* 268:25527–25535.

Lin, X., and D.L. Barber. 1996. A calcineurin homologous protein inhibits GTPase-stimulated Na-H exchange. *Proc. Natl. Acad. Sci. USA.* 93:12631–12636.

Okada, T., L. Sakuma, Y. Fukui, O. Hazeki, and M. Ui. 1994. Blockage of chemotactic peptide-induced stimulation of neutrophils by wortmannin as a result of selective inhibition of phosphatidylinositol 3-kinase. *J. Biol. Chem.* 269:3563–3567.

Orlowski, J. 1993. Heterologous expression and functional properties of amiloride high affinity (NHE-1) and low affinity (NHE-3) isoforms of the rat Na/H exchanger. *J. Biol. Chem.* 268:16369–16377.

Orlowski, J., and S. Grinstein. 1997. Na^+/H^+ exchangers of mammalian cells. *J. Biol. Chem.* 272:22373–22376.

Orlowski, J., and R.A. Kandasamy. 1996. Delineation of transmembrane domains of the Na^+/H^+ exchanger that confer sensitivity to pharmacological antagonists. *J. Biol. Chem.* 271:19922–19927.

Raucher, D., T. Stauffer, W. Chen, K. Shen, S. Guo, J.D. York, M.P. Sheetz, and T. Meyer. 2000. Phosphatidylinositol 4,5-bisphosphate functions as a second messenger that regulates cytoskeleton-plasma membrane adhesion. *Cell.* 100:221–228.

Rhee, S.G., and Y.S. Bae. 1997. Regulation of phosphoinositide-specific phospholipase C isozymes. *J. Biol. Chem.* 272:15045–15048.

Rotin, D., and S. Grinstein. 1989. Impaired cell volume regulation in Na^+-H^+ exchange-deficient mutants. *Am. J. Physiol.* 257:C1158–C1165.

Sakisaka, T., T. Itoh, K. Miura, and T. Takenawa. 1997. Phosphatidylinositol 4,5-bisphosphate phosphatase regulates the rearrangement of actin filaments. *Mol. Cell. Biol.* 17:3841–3849.

Schacht, J. 1976. Inhibition by neomycin of polyphosphoinositide turnover in subcellular fractions of guinea-pig cerebral cortex in vitro. *J. Neurochem.* 27:1119–1124.

Shannon, T.R., C.C. Hale, and M.A. Milanick. 1994. Interaction of cardiac Na-Ca exchanger and exchange inhibitory peptide with membrane phospholipids. *Am. J. Physiol.* 266:C1350–C1356.

Shrode, L.D., B.S. Gan, S.J. D'Souza, J. Orlowski, and S. Grinstein. 1998. Topological analysis of NHE1, the ubiquitous Na^+/H^+ exchanger using chymotryptic cleavage. *Am. J. Physiol.* 275:C431–439.

Silva, N.L., R.S. Haworth, D. Singh, and L. Fliegel. 1995. The carboxyl-terminal

region of the Na$^+$/H$^+$ exchanger interacts with mammalian heat shock protein. *Biochemistry*. 34:10412–10420.

Stauffer, T.P., S. Ahn, and T. Meyer. 1998. Receptor-induced transient reduction in plasma membrane PtdIns(4,5)P$_2$ concentration monitored in living cells. *Curr. Biol.* 8:343–346.

Thomas, J.A., R.N. Buchsbaum, A. Zimniak, and E. Racker. 1979. Intracellular pH measurements in Ehrlich ascites tumor cells utilizing spectroscopic probes generated in situ. *Biochemistry*. 29:2210–2218.

Varnai, B., and T. Balla. 1998. Visualization of phosphoinositides that bind pleckstrin homology domains: calcium- and agonist-induced dynamic changes and relationship to myo-[^{3}H]inositol-labeled phosphoinositide pools. *J. Cell Biol.* 143:501–510.

Wakabayashi, S., B. Bertrand, M. Shigekawa, P. Fafournoux, and J. Pouyssegur. 1994. Growth factor activation and "H$^+$-sensing" of the Na$^+$/H$^+$ exchanger isoform 1 (NHE1). Evidence for an additional mechanism not requiring direct phosphorylation. *J. Biol. Chem.* 269:5583–5588.

Weinman, E.J., D. Steplock, and S. Shenolikar. 1993. CAMP-mediated inhibition of the renal brush border membrane Na$^+$/H$^+$ exchanger requires a dissociable phosphoprotein cofactor. *J. Clin. Invest.* 92:1781–1786.

Yu, F.X., H.Q. Sun, P.A. Janmey, and H.L. Yin. 1992. Identification of a polyphosphoinositide-binding sequence in an actin monomer-binding domain of gelsolin. *J. Biol. Chem.* 267:14616–14121.

Yun, C.H.C., S. Oh, M. Zizak, D. Steplock, S. Tsao, C.M. Tse, E.J. Weinman, and M. Donowitz. 1997. cAMP-mediated inhibition of the epithelial brush border Na$^+$/H$^+$ exchanger, NHE3, requires an associated regulatory protein. *Proc. Natl. Acad. Sci. USA*. 94:3010–3015.

Zizak, M., G. Lamprecht, D. Steplock, N. Tariq, S. Shenolikar, M. Donowitz, C.H. Yun, and E.J. Weinman. 1999. cAMP-induced phosphorylation and inhibition of Na$^+$/H$^+$ exchanger 3 (NHE3) are dependent on the presence but not the phosphorylation of NHE regulatory factor. *J. Biol. Chem.* 274:24753–24758.